A New, Practical Approach to Maintaining an Efficient Yet Acceptably-performing Wireless Networked Control System

James H. Taylor* and Hazem M. S. Ibrahim†
Dep't. of Electrical & Computer Engineering
University of New Brunswick
Fredericton, N.B., CANADA E3B 5A3
*jim_taylor@ieee.org; †hazem.saad@unb.ca

***Abstract*— Wireless networked control systems have begun to gain acceptance during the last decade, due to the increased flexibility and lower costs they promise to provide compared with wired installations. The pace of application has been held back, however, by the reluctance of industry to make the accommodations necessary to allow wireless paths to be incorporated safely in process control loops, thus limiting the potential applications and benefits of wireless systems. Wireless control signals face time delay that may degrade the performance of the control loop or even lead to instability. This time delay depends on the network configuration. The sampling rate also has a great impact on the stability and performance of the closed-loop control system over the communication networks, yet the data rate should be minimized to conserve node battery life.**

The main goal of this paper is to present and discuss a real-time nonlinear control system approach that (1) checks a proposed network configuration to determine the time delay which the control data packets will encounter, and reject any proposed configuration that would lead to poor closed-loop system performance; and (2) determines the minimum acceptable sampled data rate that does not degrade control loop performance excessively. The jacketed continuous stirred-tank reactor will be presented as a typical application, to illustrate and validate this development.

***Keywords* — wireless sensor networks, wireless control loops, WSN energy conservation, control loop performance**

I. INTRODUCTION

During the past two decades, a large amount of research has been done on distributed control systems that incorporate wireless sensor networks, or what are called Wireless Networked Control Systems (WNCSs). That interest can be traced to the many advantages achieved by eliminating the costs and restrictions of traditional point-to-point wired control architectures, such as a reduction in wiring cost, rapid deployment, flexible installation, fully mobile operation, and improved freedom in placement of controllers [1] [2] [3] [4] [5]. In such systems, distributed sensors, controllers, and actuators are exchanging information over a wireless communication network.

Improved technology and stricter requirements make the development of WNCSs more difficult, however. Part of the problem arises from inflexibility in the imposition of strict requirements on data rates, latency and data loss to ensure control system performance on one hand [3] [5], and effective protocols for wireless sensor network (WSN) robustness and efficiency on the other [1] [4]. Our primary interest in WNCSs is for Petroleum Applications of Wireless Systems (PAWS[1]), a major research program at Cape Breton University (CBU, the project lead organization that deals with WSNs [5] [6]) and the University of New Brunswick (UNB, focussed on Intelligent Control and Asset Management or ICAM [7]).

WSN data rates affect both the performance of a control system implemented with wireless communication links in its closed loops and the WSN nodes' energy consumption. The main goal of this paper is to present a pragmatic way to determine the minimum data rates (maximum sampling times τ_{s-max}) that maintain adequate performance of the closed loop control system, thus allowing the energy consumption of the WSN nodes to be reduced to the extent possible.

As is well known, the value of τ_{s-max} depends on the data delays or latencies τ_d introduced in the control loop paths by the WSN; this, in turn, depends on the WSN configuration, especially the number of hops in these paths. If we account for delay via a conservative (worst-case) design, based, for example, on the maximum number of hops and the maximum delay per hop, then an unreasonably small τ_{s-max} may be demanded; this we wish to avoid. Therefore, we assume that τ_d can be determined experimentally for the WSN configuration in use, by using either time stamps, 'ping' tests or counting hops. WSN reconfiguration will obviously require a redetermination of τ_d and $\tau_{s-min}(\tau_d)$, so the approach should be relatively easy to execute and fast.

The UNB team has developed a Wireless Networked Control System Coordination Agent (WNCSCA), which is responsible for assigning and managing the WSN data rates as well as accepting or rejecting the configuration of the WSN based on delays in the control-loop paths over the WSN. Both of these factors have a major impact on controller performance, and the WNCSCA will not only maintain the stability of the closed-loop control system but also guard against the performance of the closed loop control system degrading excessively. On the other hand, node energy conservation is a critical issue in WSNs in terms of node and network life, as the nodes are usually powered by batteries, and in many cases the replacement of these power sources is difficult, inconvenient, and/or expensive. Our WNCSCA coordinates with ICAM and the WSN Gateway to allow as much network optimization and flexibility as possible under constraints imposed by the WNCS requirements.

II. WNCS COORDINATION AGENT

Our WNCSCA is being implemented as a part of ICAM, which is a multi-agent intelligent supervisory system for petroleum processing facilities [7]. This agent will mediate between the ICAM system and the Gateway of CBU's Wireless Industrial Sensor Network Testbed For Radio-Harsh

[1]The Petroleum Applications of Wireless Systems project is supported by the Government of Canada, through the Atlantic Innovation Fund (AIF).

Environments (WINTeR), which is an open-access, multi-user experimental testbed, developed under the PAWS project, to support implementation and evaluation of WSNs for industrial applications [6]. WINTeR now supports process simulations with wireless in the loop; in the future the goal is to interface WINTeR with actual industrial processes as well. There are two process simulators currently linked to WINTeR, one a high-order, highly complex model of a three-phase crude-oil separator [8] which has five control loops, and the other a simpler model of a jacketed continuous stirred-tank reactor (JCSTR) [9]. The JCSTR has been chosen and implemented as a process simulator to better allow the study of issues related to the stability and performance of control systems over a WSN; this will facilitate development of the WNCSCA, thus forming an important enabling technology for the use of WSNs in process control applications.

During the operation of the ICAM system, its controllers and agents may require different levels of service from the WSN to complete their functions properly. These agents include Fault Detection, Isolation and Accommodation (FDIA) [11], Nonlinear Dynamic Data Reconciliation (NDDR) [12], Linearized Model Identification (LMId) [13] and other subsidiary functions. For example, the controllers require different data rates from specific sensors and actuators in specific regimes, such as start-up, set point changes and steady state operation. During start-up and set point changes, the process variable transients must decay properly under closed-loop control, so appropriate data rates and path delays must be imposed. Once the process reaches the desired steady-state set-point the LMId agent perturbs the plant with pseudo-random signals (to excite all the modes in the plant), gather data and apply its model identification algorithm, perhaps needing a different data rate than before. After that, the process may remain settled in steady state, in which case loops can be opened[2] and data rates substantially reduced so ICAM can monitor the process; as long as there are no disturbances or set-point changes slow sampling can continue and the WSN Gateway can manage its operations freely and conserve energy accordingly. Alternatively, if FDIA is to continue during steady state (and that would most likely be desirable) data rates can be reduced somewhat, but not as much as passive monitoring would allow. In many industrial systems a process may be in steady state for long periods of time, with infrequent set-point changes requiring closed-loop control, so this strategy will allow the WSN to be managed in a more energy-efficient manner much of the time. A communication protocol for the WNCSCA is developed and presented in [14]; in this paper we focus on issues relating to the management of time delay and sampling rate.

In summary, the various modes of operation require tighter or looser constraints on data rates and control signal path delays; the WNCSCA mediates between ICAM and the WSN Gateway to allow both the control system and the WSN to meet their objectives as flexibly and effectively as possible.

III. JCSTR Process Simulation Model

The ICAM system processes real-time data that are collected from either an external plant or from a real-time process simulation model which reproduces the nonlinear nature of a typical petroleum application plant. UNB's real-time JCSTR simulator is embedded in WINTeR at Cape Breton University to permit running experiments with wireless-in-the-loop. The physical characteristics, modeling and simulation of the JCSTR are outlined in the following sections.

[2]Opening control loops momentarily to handle data drop-outs has been suggested in [3]; we believe that our strategy of opening control loops during steady-state operation to remove strict control-related WSN constraints is new.

A. Nonlinear JCSTR simulator

The JCSTR simulator was implemented as both a MATLAB® function [9] (encoding the vector differential equations for the nonlinear JCSTR including the PI controller, suitable for use with MATLAB® integrators such as `ode45`) and as a Simulink® model (with the physical process modeled as MATLAB® code in an S function, digital controller blocks, delay elements and zero-order holds). A schematic of the JCSTR is depicted in figure 1. As shown, the tank inlet or "mixture" flow is received from another process unit. There is also a heating fluid circulated through the jacket in order to heat the mixture inside the tank. The main objective of the JCSTR is to control the mixture level (via the level controller or **LC**) and the mixture temperature (via the temperature controller or **TC**) inside the tank reactor. This is done by controlling the jacket inlet valve flow rate and the tank outlet valve flow rate.

The following assumptions were made in order to derive the dynamic modeling equations of the tank and jacket:

- Liquids have constant density and heat capacity.
- Mixing in both the tank and the jacket is ideal.
- The amount of liquid in the jacket is constant, i.e., $F_{jin} = F_{jout}$.
- The tank inlet flow rate, tank inlet temperature and jacket inlet temperature may change; these are uncontrolled inputs.
- The tank outlet flow rate and jacket flow rate are control inputs (actuation).
- The rate of heat transfer from the jacket to the tank is governed by $Q = U\,A_H\,(T_j - T)$, where U is the overall heat transfer coefficient and A_H is the area for heat transfer, $A_H = A_B + \pi DH$ where A_B is the area of the base, D is the diameter of the base and H is the height of the mixture.

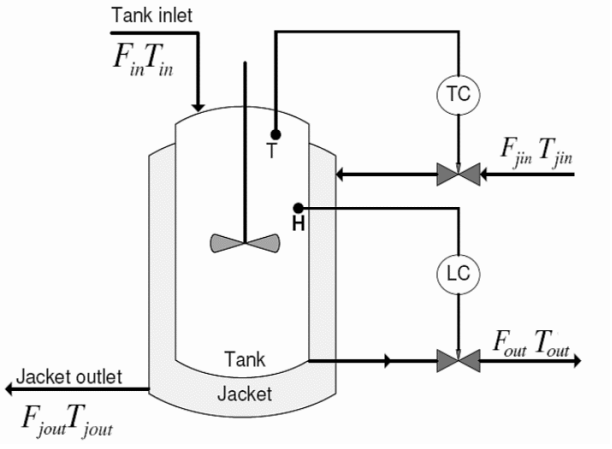

Fig. 1. Jacketed continuously stirred-tank reactor.

The JCSTR process is described by a third-order model which has two control inputs, three state variables, and two controlled variables. Specifically, the **state variables** are mixture height, H, mixture temperature, T, and the jacket temperature, T_j; $x = [\,H\;\;T\;\;T_j\,]^T$. The **input variables** are divided into two

groups: **control inputs**, i.e., mixture outflow, F_{out}, and jacket inflow, F_{jin}; $u = [\, F_{out} \;\; F_{jin} \,]^T$; and **exogenous inputs**, viz. mixture inflow, F_{in}, temperature of the mixture feed, T_{in}, and temperature of the jacket inflow, T_{jin}; $w = [\, F_{in} \;\; T_{in} \; T_{jin} \,]^T$. Finally, the JCSTR outputs are the controlled variables H and T; $y = [\, H \;\; T \,]^T = [\, x_1 \;\; x_2 \,]^T$. The exogenous inputs may be regarded as disturbances; here we consider them to be constant.

The following ordinary differential equations describe the dynamic behavior of the JCSTR:

$$\begin{aligned} \dot{H} &= \frac{1}{A_B}(F_{in} - F_{out}) \\ \dot{T} &= \frac{F_{in}(T_{in} - T)}{A_B H} + \frac{U A_H (T_j - T)}{\rho\, C_p A_B H} \\ \dot{T_j} &= \frac{F_{jin}(T_{jin} - T_j)}{V_j} - \frac{U A_H (T_j - T)}{\rho\, C_p V_j} \end{aligned} \tag{1}$$

where the subscripts in, out, j refer to inlet, outlet and jacket respectively. In addition to the parameters defined above, we have ρ = mixture density, C_p = heat capacity of the mixture and V_j = jacket water volume. The values of the JCSTR model parameters are provided in [9]. Note that the size of the unit has a major impact on the system time constants; here we use normalized units for level and time, i.e., both variables are given in *per unit (pu)* rather than meters and minutes.

B. Controller design for the JCSTR

Linearization about the set point has been used in order to design a controller for this nonlinear system. Most process control systems are required to keep the states of the dynamic process at specific constant values or set points. This is achieved by providing control signals (plant inputs) that have two components: The first part or **feedforward term** $\bar{u}$ generates the control signal needed to keep the process at the set point in steady state, and the second component or **feedback term** δu generates the incremental control needed to return the process to the set point if it should deviate from it [10]. The structure of the control system designed in this way is shown in figure 2.

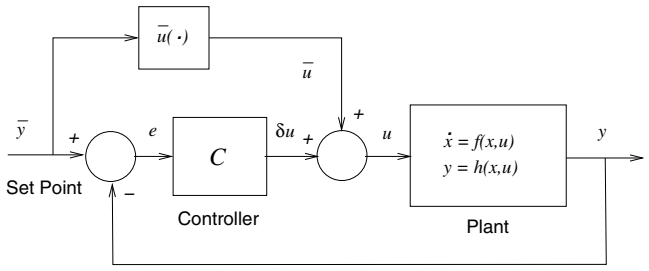

Fig. 2. Control system structure, linearization about a set point.

The steady-state control component can be determined as follows: Given a nonlinear process,

$$\dot{x} = f(x,u)\,, \quad y = g(x,u) \tag{2}$$

Suppose that $\bar{y}$ is the set point or desired output for the control system, which is assumed to be constant. Suppose also that $\bar{x}$ and $\bar{u}$ are the steady-state values of the state and control, respectively, that produce this constant output. Since $\bar{x}$ is thus an equilibrium state we have $\dot{x} = 0$, so we have to solve a set of algebraic equations,

$$0 = f(\bar{x},\bar{u})\,, \quad \bar{y} = g(\bar{x},\bar{u}) \tag{3}$$

For the JCSTR we have $\bar{y} = [\, \bar{x}_1 \;\; \bar{x}_2 \,]^T$ with given set-point values, and $\bar{x}_3$, $\bar{u}_1$ and $\bar{u}_2$ as unknowns, so this is a well-posed problem involving the solution of three simultaneous equations ($f(\bar{x},\bar{u}) = 0$) in three unknowns.

The feedback controller operates on the **error** or difference between the desired output $\bar{y}$ and the actual output y to generate a corrective control signal δu. Then, the corrective control signal is summed with the feedforward control signal $\bar{u}$ to produce the actual control signal u as input to the plant.

Substituting the previous definitions of x and u into eqns. (1) we can write the three state differential equations as:

$$\begin{aligned} \dot{x_1} &= \frac{1}{A_B}(F_{in} - u_1) \\ \dot{x_2} &= \frac{F_{in}(T_{in} - x_2)}{A_B x_1} + \frac{U(x_3 - x_2)}{\rho\, C_p\, x_1} + \frac{U\pi D(x_3 - x_2)}{\rho\, C_p A_B} \\ \dot{x_3} &= \frac{u_2(T_{jin} - x_3)}{V_j} - \frac{U A_B (x_3 - x_2)}{\rho\, C_p\, V_j} - \frac{U\pi D x_1 (x_3 - x_2)}{\rho\, C_p\, V_j} \end{aligned} \tag{4}$$

Therefore, the equilibrium conditions using eqn. (3) are:

$$\begin{aligned} \bar{u}_1 &= F_{in} \\ \bar{u}_2 &= \frac{F_{in}(\bar{x}_2 - T_{in})}{T_{jin} - \bar{x}_3} \\ \bar{x}_1 &= \bar{y}_1 = \text{set point 1 (given)} \\ \bar{x}_2 &= \bar{y}_2 = \text{set point 2 (given)} \\ \bar{x}_3 &= \bar{x}_2 + \frac{F_{in}\rho C_p(\bar{x}_2 - T_{in})}{U A_B + U\pi D \bar{x}_1} \end{aligned} \tag{5}$$

The second and fifth relations can be solved to obtain

$$\bar{x}_3 \;=\; \bar{x}_2 + \frac{F_{in}\,(\bar{x}_2 - T_{in})}{\alpha\,(A_B + \pi D_r \overline{x}_1)} \tag{6}$$

$$\bar{u}_2 \;=\; \frac{F_{in}\,(\bar{x}_2 - T_{in})}{T_{jin} - \bar{x}_3} \tag{7}$$

As mentioned, we used small signal linearization to design the feedback controller C which regulates the system to maintain its output at the desired set point. This procedure is well known, so we merely refer to [9] for the (A, B, C, D) array elements in the usual linearized model formulation.

We converted the linearized state space formulation to its equivalent transfer function form, and designed a suitable diagonal 2×2 PI controller that gives a fast response with moderate overshoot.

C. JCSTR simulator benchmark

In order to establish the process simulator's ideal performance under digital control, with no delay and fast sampling time $\tau_s = 0.1\ pu$, step changes are applied to the set points for the level and the temperature of the mixture inside the tank reactor. Specifically, we start with the initial conditions of the states being $x_{10} = 0.66\,pu$, $x_{20} = 50\,C$, and $x_{30} = 143\,C$, and apply two successive set-point changes for the level and the temperature inside the reactor. The level set point changes at $t = 1.8\,pu$ from $0.7\,pu$ to $0.75\,pu$. The mixture temperature set point changes at $t = 2.4\,pu$ from $52\,C$ to $56\,C$. The step responses of these changes in the set points are shown in figures 3 and 4, respectively. The corresponding benchmark percent overshoots (% OSs) are 10.8 for the level loop and 11.0 for the mixture temperature loop.

Changing the sampling time: The sampling time τ_{s-LC} of the mixture level sensor was varied to check its effect

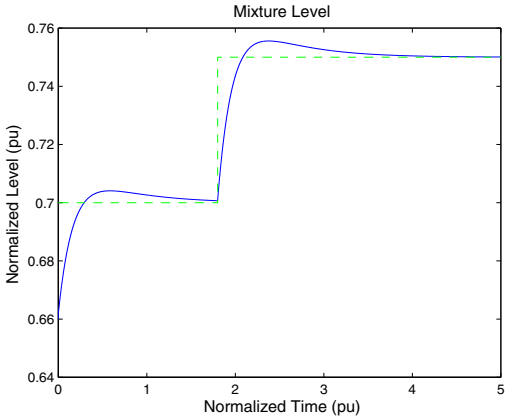

Fig. 3. Mixture level vs normalized time.

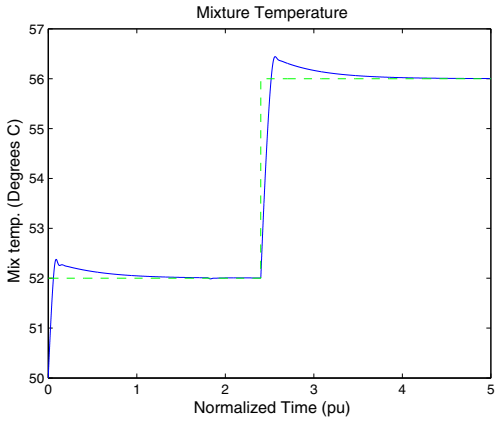

Fig. 4. Mixture temperature vs normalized time.

on closed loop control performance. Note that we do not merely insist on stability, we establish a threshold of acceptable percent overshoot, here taken to be 25%. By iteratively adjusting τ_{s-LC}, we found that the minimum sampling rate that keeps the mixture level control performance acceptable in this sense is $0.25\ pu$, which gives 24.9 % OS, as shown in figure 5. Of course, more conservative values of % OS can be mandated, e.g., benchmark % OS = 0, maximum acceptable % OS = 10. The same method was applied to the mixture

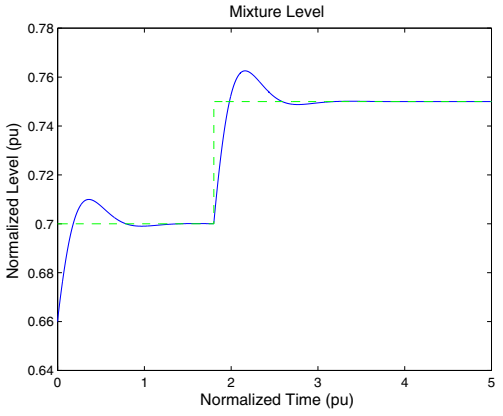

Fig. 5. Mixture level vs normalized time, $\tau_{s-LC} = 0.25\ pu$ (24.9% OS).

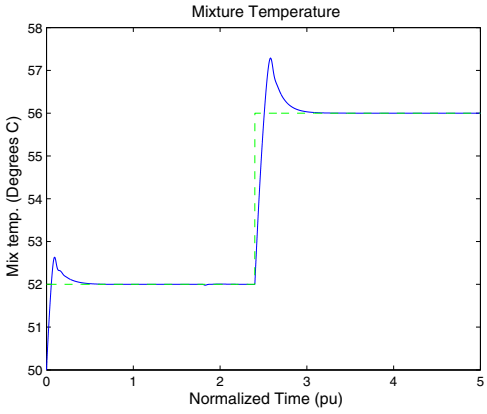

Fig. 6. Mixture temperature vs normalized time, $\tau_{s-TC} = 0.3\ pu$ (28.5% OS).

temperature control loop. By changing the sampling time for the mixture temperature sensor, τ_{s-TC}, we found that the maximum sampling rate that produces acceptable % OS is 0.3 pu, which yielded 28.5% OS, as shown in figure 6.

Adding time delay elements: The effect of delay was studied by resetting the sampling rates to their benchmark values and inserting time-delay elements in the feedback paths of the level and temperature loops. By increasing the time delay elements gradually starting from zero time delay, we can find the maximum time delays τ_{dL-max} and τ_{dT-max} which lead to marginally acceptable performance. Running the above experiment for both loops, we found that the maximum time delay for the level control loop is $\tau_{dL-max} = 0.253\ pu$, which gives 25% OS, and the maximum time delay element for the temperature control loop is $\tau_{dT-max} = 0.1\ pu$ for a slightly larger % OS, as shown in figures 7 and 8.

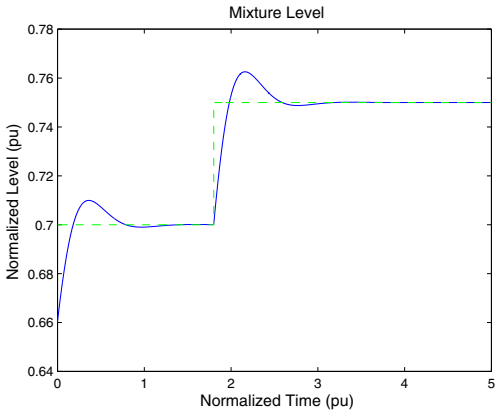

Fig. 7. Mixture level vs normalized time, $\tau_d = 0.253\ pu$ (25% OS).

D. Sampling time and maximum delay time relationship

Another case study has been performed to show the relationship between the sampling times and the maximum time delays that produce acceptable closed-loop control for our WNCS. We fixed the sampling rate and delay time of the temperature sensor at three operating points, as shown in figure 9, varied the sampling time of the level sensor, and plotted the curves of τ_{dL-max} versus τ_{s-LC} for each case. The expected inverse relationship between the sampling time and the maximum time

delay for % OS $\leq$ 25 has been determined, as shown in that figure. These plots also reveal the interactive nature of these two loops.

This study was also reversed, by fixing the sampling rate and delay time of the level sensor at three operating points, varying the sampling time of the temperature sensor, and plotting the curves of τ_{dT-max} versus τ_{s-TC} for each case; here, too, we observed a similar relationship and interaction between the two loops.

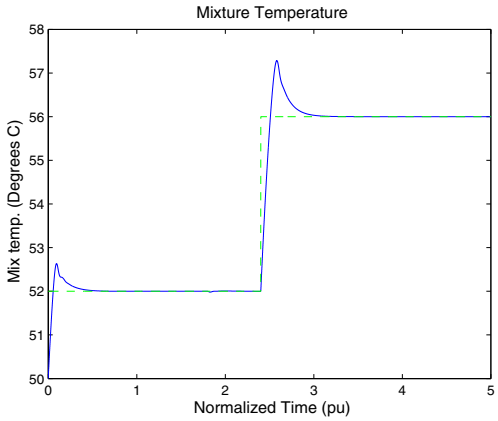

Fig. 8. Mixture temperature vs normalized time, $\tau_d = 0.186$ pu (28.9% OS).

These experiments illustrate the relationship between different sampling times for each sensor and their corresponding maximum time delay which makes the closed-loop control system perform acceptably. They served as the basis for the strategy presented next.

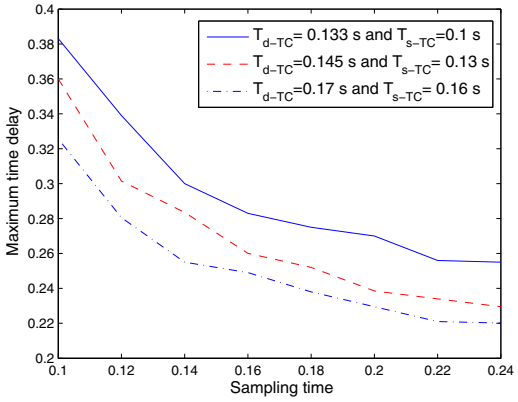

Fig. 9. Maximum delay time and sampling time relationship for the level control loop.

E. Proposed WNCSCA *strategy*

Based on the observations presented above, we have adopted the following strategy for determining appropriate minimal sampling rates for the WNCS:

1) Consider a WSN configuration proposed by the Gateway, and determine the control path delays by either using time stamps, 'ping' experiments, or simply multiplying the actual number of hops by an estimated delay-per-hop.
2) Accept the proposed configuration conditionally if its control path delays are less than the τ_{d-max} determined for the benchmark sampling rates, otherwise reject it and request a new proposal.
3) Find the minimum sampling rate (i.e., τ_{s-max}) for the two loops by the method of successive approximation, as follows:
   a) Fix τ_{s-LC} at its benchmark value and τ_{d-LC} corresponding to that determined for the proposed configuration; find $\tau_{sT}(1)$ such that acceptable % OS is achieved; an iterative approach that successively doubles the ideal sampling time τ_{si} until the % OS limit is violated, halves the last interval and checks again to see if acceptable % OS is achieved; continue halving and increasing/decreasing τ_s until % OS is within a specified tolerance ϵ_{OS} of the limit, as shown in figure 10 (in this illustration the trial values of τ_{sT} were $2\tau_{si}$, $4\tau_{si}$, $8\tau_{si}$ and finally $7\tau_{si}$);
   b) Fix $\tau_{s-TC} = \tau_{sT}(1)$ and τ_{dT} corresponding to the proposed configuration; find $\tau_{sL}(1)$ such that acceptable % OS is achieved;
   c) Fix $\tau_{s-LC} = \tau_{sL}(1)$ and τ_{dL} corresponding to the proposed configuration; find $\tau_{sT}(2)$ such that acceptable % OS is achieved;
   d) Iterate in this way until the % OS for τ_{sL_k} and $\tau_{sL\_(k-1)}$ differ by less than a tolerance ϵ_L; stop. (The stopping criterion can be applied to either loop.)

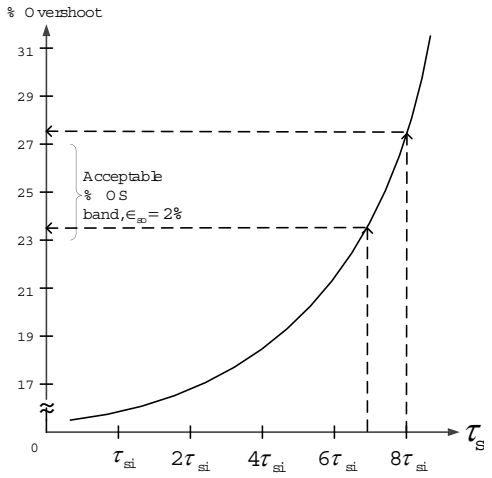

Fig. 10. Determining the maximum sampling time for the TC loop.

We illustrate applying the successive approximation method to the level and temperature control loops of our JCSTR simulator as follows: Assume that the Gateway determined the control path delays to be 0.17 and 0.1 pu for the level and temperature control loops, respectively. Assume that point A in figure 11 corresponds to $\tau_{sT}(1)$ for the temperature control loop which yields 25 % OS resulting from fixing the level loop at its benchmark values for the sampling time and the time delay. By fixing the temperature loop control system to operate at point A, which has $\tau_{sT}(1)$ = 0.185 pu and τ_{dT} = 0.10 s, and varying the sampling time of the level sensor, τ_{sL}, we can plot the curve of time delay vs. sampling time (the "point

A conditions" curve, as shown in figure 12). The "Point A conditions" curve cuts the time delay line τ_{dL} = 0.17 pu at point B, yielding $\tau_{sL}(1) = 0.11pu$. The temperature % OS for point B has been determined to be 27.2 %, which is too high, so we need iterate again. By repeating the above method,

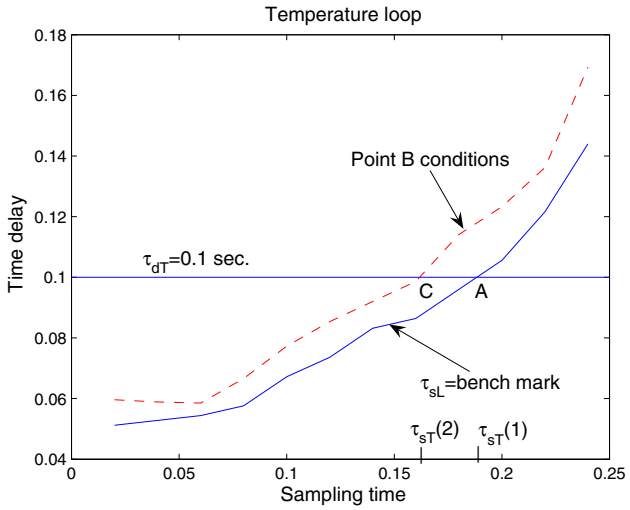

Fig. 11. Determining the maximum sampling time for the TC loop.

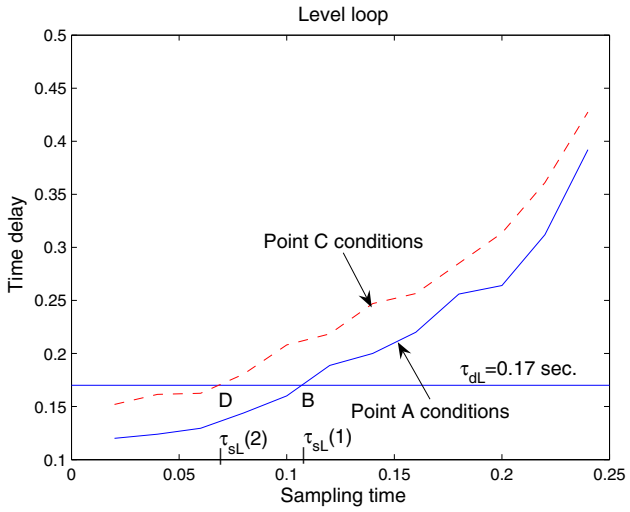

Fig. 12. Determining the maximum sampling time for the TC loop.

fixing point B which has $\tau_{sL}(1)$ = 0.11 pu and τ_{dL} = 0.17 pu and varying the sampling time of the temperature sensor, and plotting the curves of sampling time and time delay (the "point B conditions" curve), as shown in figure 11, we see that the "point B conditions" curve cuts the time delay line τ_{dT} = 0.1 pu at point C. By fixing the temperature loop control system to operate at point C, which has $\tau_{sT}(2)$ = 0.16 pu and τ_{dT} = 0.10 pu and varying the sampling time of the level sensor, and plotting the curves of sampling time and time delay (the "point C conditions" curve), as shown in figure 12, we determine that setting $\tau_{sL}(2)$ = 0.071 (point D) the % OS of the two loops are 24.3 % and 25 %, respectively, which are quite acceptable performance (according to our criterion) and we can stop the iterations.

By using the above strategy the WNCSCA determines τ_{s-max} for both the level loop and the temperature loop in an efficient and fast way. The above strategy will achieve very good performance in terms of simulation time when the WNCSCA controls a process with a higher number of interacting loops, such as the pilot plant simulator that represents an oil production facility, which separates oil well fluids into crude oil, sales gas, and water which has five loops. The plant itself is at the College of the North Atlantic (CNA) [16], and may be used in future PAWS research.

IV. Conclusion

Sampling times and time delays play a vital role in the performance of industrial WNCSs. A nonlinear JCSTR simulator model has been implemented to test and understand these issues. The reduction of the sampling frequencies for the wireless sensor network's nodes increases their batteries' life, but there are strict limits to this reduction which conflicts with the performance of closed-loop control. A proposed Wireless Networked Control System Coordination Agent manages this potential "conflict of interest" between industrial control systems requirements and objectives of a typical wireless sensor network to satisfy control and WSN requirements to the extent possible.

V. ACKNOWLEDGMENTS

This project is supported by Atlantic Canada Opportunities Agency (ACOA) under the Atlantic Innovation Fund (AIF) program. The authors gratefully acknowledge that support and the collaboration of the Petroleum Applications of Wireless Systems (PAWS) team at CBU.

References

[1] C. Fischione, K. H. Johansson, F. Graziosi, and F. Santucci. Distributed cooperative processing and control over wireless sensor networks. *Proc. International Conference on Wireless Communications and Mobile Computing* . July 2006.
[2] P. Kawka and A. Alleyne. Stability and feedback control of wireless networked systems. *Proc. American Control Conference*. June 2005.
[3] X. Liu and A. Goldsmith. Wireless network design for distributed control. *Proc. 43rd IEEE Conference on Decision and Control*, December 2004.
[4] N. Plopyls, P. Kawka, and A. Alleyne. Closed-loop control over wireless networks. *IEEE Control Systems magazine*, June 2004.
[5] I. Johnstone, J. Nicholson, B. Shehzad, and J. Slipp. Experiences from a wireless sensor network deployment in a petroleum environment. *ACM International Wireless Communications and Mobile Computing Conference (IWCMC)*, August 2007.
[6] J. Slipp, C. Ma, M. Murillo, J. Nicholson, N. Polu, and S. Hussain. WINTeR: architecture and applications of a wireless industrial sensor network testbed for radio-harsh environments. *Proc. Communication Networks and Services Research*, January 2008.
[7] J. Taylor and A. Sayda. Prototype design of a multi-agent system for integrated control and asset management of petroleum production facilities. *Proc. American Control Conference*, June 2008.
[8] A. Sayda and J. Taylor. Modeling and control of three-phase gravity separators in oil production facilities. *Proc. American Control Conference*, July 2007.
[9] J. Taylor. Jacketed Continuous Stirred-tank Reactor - Models, Control Systems and Simulators, PAWS Internal Memo (available from the author
[10] B. Friedland. Advanced control system design. *Prentice-Hall, Inc*. 1995.
[11] J. H. Taylor and M. Omana. Fault Detection, Isolation and Accommodation Using the Generalized Parity Vector Technique. *Proc. IFAC World Congress*, July 2008.
[12] J. H. Taylor and M. Laylabadi. A Novel Adaptive Nonlinear Dynamic Data Reconciliation and Gross Error Detection Method. *Proc. IEEE Conference on Control Applications*, October 2006.
[13] Maira Omana, *Fault Detection, Isolation and Accommodation Using the Generalized Parity Vector Technique*. UNB PhD thesis, October 2009.
[14] J. H. Taylor, H. M. S. Ibrahim and J. Slipp, "Proposal and Communication Scheme for a Wireless Networked Control System Coordination Agent". *submitted to International Conference on Cyber-Physical Systems, Stockholm, Sweden*. 12-16 April 2010.